

# In Vitro Antiviral Activity of *Cinnamomum cassia* and Its Nanoparticles Against H7N3 Influenza A Virus

Munazza Fatima<sup>1</sup>, Najam-us-Sahar Sadaf Zaidi<sup>1\*</sup>, Deeba Amraiz<sup>1</sup>, and Farhan Afzal<sup>2</sup>

<sup>1</sup>Atta-ur-Rahman School of Applied Biosciences (ASAB), National University of Sciences and Technology (NUST), H-12, Kashmir Highway, Islamabad, Pakistan

<sup>2</sup>Disease Diagnostic Section, Poultry Research Institute, Rawalpindi, Pakistan

Received: August 10, 2015  
Revised: September 9, 2015  
Accepted: September 23, 2015

First published online  
September 25, 2015

\*Corresponding author  
Phone: +92-51-9085-6132;  
Fax: +92-51-9085-6102;  
E-mail: zaidi.sahar@gmail.com

pISSN 1017-7825, eISSN 1738-8872

Copyright© 2016 by  
The Korean Society for Microbiology  
and Biotechnology

Nanoparticles have wide-scale applications in various areas, including medicine, chemistry, electronics, and energy generation. Several physical, biological, and chemical methods have been used for synthesis of silver nanoparticles. Green synthesis of silver nanoparticles using plants provide advantages over other methods as it is easy, efficient, and eco-friendly. Nanoparticles have been extensively studied as potential antimicrobials to target pathogenic and multidrug-resistant microorganisms. Their applications recently extended to development of antivirals to inhibit viral infections. In this study, we synthesized silver nanoparticles using *Cinnamomum cassia* (Cinnamon) and evaluated their activity against highly pathogenic avian influenza virus subtype H7N3. The synthesized nanoparticles were characterized using UV-Vis absorption spectroscopy, scanning electron microscopy, and Fourier transform infrared spectroscopy. Cinnamon bark extract and its nanoparticles were tested against H7N3 influenza A virus in Vero cells and the viability of cells was determined by tetrazolium dye (MTT) assay. The silver nanoparticles derived from Cinnamon extract enhanced the antiviral activity and were found to be effective in both treatments, when incubated with the virus prior to infection and introduced to cells after infection. In order to establish the safety profile, Cinnamon and its corresponding nanoparticles were tested for their cytotoxic effects in Vero cells. The tested concentrations of extract and nanoparticles (up to 500 µg/ml) were found non-toxic to Vero cells. The biosynthesized nanoparticles may, hence, be a promising approach to provide treatment against influenza virus infections.

**Keywords:** Antiviral activity, nanoparticles, H7N3, influenza, *Cinnamomum cassia*, cinnamon bark

## Introduction

New applications of nanomaterials and nanoparticles are emerging rapidly [13]. Nanoparticles can be prepared by a variety of methods such as chemical reduction [11], bioreduction [50], electrochemical reduction [22, 24], photochemical reduction [45], and heat evaporation [55, 58]. Biological methods for the synthesis of nanoparticles using enzymes [18], microorganism [9, 10], and plants or plant extracts [1, 47] can be advantageous over chemical and physical methods as they are eco-friendly and cost effective, and can be scaled up easily for large-scale production.

Nanoparticles are being explored extensively in the field of medicine. As the size of nanoparticles is similar to that of biological molecules, this makes them a promising candidate for application in both in vivo and in vitro research [31]. Metallic nanoparticles have been studied as potential antimicrobials to target highly pathogenic and multidrug-resistant microorganisms. Their applications are being extended further to the development of antivirals to inhibit numerous viruses [16, 33].

Influenza viruses are enveloped, negative-sense RNA viruses belonging to family *Orthomyxoviridae*. These viruses are prevalent in nature and can infect all species of birds,

many mammalian species such as horses, pigs, and seals, and humans [60]. Confirmed cases of human infections caused by various subtypes of avian influenza viruses such as H5N1, H7N7, and H9N2 have been reported [32, 53]. These viruses pose a high risk to human and animal health. Avian influenza viruses usually contain hemagglutinin (HA) having Gln226 and Gly228 residues, which form a narrow receptor binding pocket that prefers 2,3-sialic acid binding. Human species generally contain Leu226 and Ser228, forming a broad pocket that favors 2,6-sialic acid binding [15, 41]. Avian influenza viruses need a switch in preferential binding of the HA protein from 2,3-sialic acid to 2,6-sialic acid, to induce a pandemic.

Antiviral drugs offer the primary line of defense for an influenza virus pandemic, where vaccines might be not accessible in time [40]. Currently approved anti-influenza drugs are inhibitors of viral M2 ion channel (amantadine and rimantadine) and viral neuraminidase (oseltamivir or zanamivir) [61]. These drugs are often limited owing to their toxicity or the appearance of mutant forms of the virus resistant to drugs [28]. Given the limited capability of currently available anti-influenza drugs, there is a need to develop new drugs that would exploit alternate modes of action and offer broad-spectrum cross-strain therapeutic cover.

Extensive work has been carried out to develop newer drugs from both natural and synthetic sources. However, the drugs from natural origin are considered to be safer because of their minimal adverse drug reactions. Hundreds of thousands of plant species have been studied for their medicinal properties [26, 42]. Many plants have been shown to possess anti-influenza activity. These include *Allium fistulosum* [34], *Pinus thunbergia* [20], *Ephedrae herba* [49], *Sambucus nigra* [14], *Alpinia katsumadai* [29], and *Psidium guajava* [2].

Plant-based silver nanoparticles (AgNPs) are a likely source of new antiviral agents because of their multi-targeting mechanism of action. Plants are readily available, have low cost, are easy to handle and nontoxic, and have a variety of metabolites that can assist reduction of silver ions [59]. Several groups reported the synthesis of Au, Ag, and Pd nanoparticles using plant extracts such as *Geranium* leaf [44], *Aloe vera* [46], lemongrass [8], tamarind leaf [13], and others [4, 19]. Metal nanoparticles have been studied for their antiviral potential and have proven to be antiviral agents against hepatitis B virus [27], respiratory syncytial virus [35], human immunodeficiency virus type 1 (HIV-1) [62], herpes simplex virus type 1 [25, 30], Tacaribe virus [63], monkeypox virus [54], and influenza virus [39, 43].

Emerging and re-emerging influenza infections demand additional antiviral strategies against influenza. Cinnamon has a long history both as a medicine and spice [3]. Little is known about the anti-influenza activity of Cinnamon and synthesis of AgNPs from Cinnamon have not been reported earlier. In the present study, green synthesis of AgNPs using aqueous extract of Cinnamon bark is reported. Furthermore, the activity of Cinnamon bark and its corresponding nanoparticles was evaluated against highly pathogenic avian influenza virus subtype H7N3 in Vero cells.

## Materials and Methods

### Viral Propagation in Eggs

The field isolates of avian influenza virus H7N3 were obtained from the Disease Diagnostic Section, Poultry Research Institute, Rawalpindi, Pakistan. The virus was propagated in 9-day-old embryonated chicken eggs. After 24 h of inoculation, the allantoic fluid was harvested and a hemagglutination test was performed to quantify the virus. The virus was then used for the infectivity assay.

Vero cells were obtained from the Microbiology Laboratory, University of Veterinary and Animal Sciences, Lahore, Pakistan. Cells were maintained in Dulbecco's modified Eagle's medium (DMEM) supplemented with 10% fetal bovine serum, 2 mM L-glutamine, 100 U/ml penicillin, and 100 µg/ml streptomycin and incubated at 37°C under 5% CO<sub>2</sub>. Cells were monitored daily for confluency and passaged into a new tissue culture flask when they reached >90% confluency. They were used for antiviral assay on the 14<sup>th</sup> passage.

### Preparation of Plant Extract and Nanoparticles

Commercially available, highest grade Cinnamon bark was obtained from Fateh Food International, Pakistan. Cinnamon bark was grinded and passed through a sieve of 50/80 mesh to obtain fine powder. Then, 25 g of powder was weighed and added into 100 ml of deionized water. The Cinnamon aqueous extract was filtered with Whatman No. 1 filter paper (pore size 25 µm) and 10 ml of this extract was added into 90 ml of 1 mM silver nitrate (AgNO<sub>3</sub>) solution and kept at room temperature for 5 h for reduction of silver (Ag<sup>+</sup>) ions. AgNPs synthesis in the reaction mixture containing AgNO<sub>3</sub> and Cinnamon extract was observed by color change.

### Physicochemical Characterization of Nanoparticles

A small aliquot of the prepared silver nanoparticles was diluted with deionized water and subjected to UV-Vis spectral analysis on a spectrophotometer (Model UVD-2950; USA) in the wavelength range of 250–550 nm. The absorbance of Cinnamon aqueous extract and corresponding NPs was measured and plotted against wavelength. The AgNP suspension was centrifuged at 16,350 ×g for 15 min. The AgNP pellet was washed with deionized water three times to remove impurities and dried.

The shape and size of the nanoparticles were determined by scanning electron microscopy (SEM; JSM-6490; USA). A drop of NP suspension was placed on a specimen chamber and coated with an ultra-thin layer of gold by a sputter coater and mounted on a specimen stub in the scanning electron microscope. Images were captured at 50,000× magnification. Then, Fourier transform infrared spectroscopy (FTIR) measurements were performed to obtain information about the possible chemical groups responsible for the reduction of ions and stability of AgNPs. Cinnamon aqueous extract and Cinnamon-based AgNPs were heated with potassium bromide (KBr) in 100:1 ratio at 110°C for 10–15 min. KBr pellets were made by a hydraulic press and placed in a sample chamber of a FTIR spectrometer (Perkin Elmer Spectrum, USA). Measurements were carried out by scanning in the spectral range of 500–4,000 cm<sup>-1</sup> with a resolution of 1 cm<sup>-1</sup>.

#### Determination of 50% Tissue Culture Infectious Dose

Vero cells were seeded into a 96-well plate (100 µl/well) at a concentration of 5 × 10<sup>4</sup> cells/ml and incubated for 24 h at 37°C under 5% CO<sub>2</sub>. H7N3 influenza virus was diluted serially in 10-fold from 10<sup>-1</sup> to 10<sup>-9</sup> and each dilution was titrated into a 96-well plate with six wells per dilution. A few wells were left as negative control having no virus. Plates were incubated at 37°C under 5% CO<sub>2</sub> and the cytopathic effect in each well was observed for 7 days. The 50% tissue culture infectious dose (TCID<sub>50</sub>) was calculated by the Reed and Muench method [5].

#### Cytotoxicity Assay

In order to perform the cytotoxicity analysis, 100 µl of cells was seeded in each well of 96-well plates at a density of 5 × 10<sup>4</sup> cells/ml. After 24 h of incubation, these cells were treated with 100 µl of various concentrations of Cinnamon bark extract and its silver nanoparticles (500, 250, 125, 62.5, 31.25, and 15.62 µg/ml). A 100 µl volume of 2% FBS-DMEM was taken as the negative control. Cells were incubated at 37°C under a 5% CO<sub>2</sub> environment for an additional 48 h. Then, MTT (3-[4,5-dimethylthiazol-2-yl]-2,5-diphenyl tetrazolium bromide) was prepared at a concentration of 5 mg/ml and 100 µl was added to each well. Plates were incubated at 37°C under 5% CO<sub>2</sub> for 4 h. Next, the reagent was removed and 100 µl of DMSO was added to each well in order to dissolve purple-color formazan crystals. Then, the optical density was measured at 540 nm using a microplate reader (ELx 800; BioTek). The cell viability was determined from the optical density values using the formula

$$\frac{\text{Control OD (untreated)} - \text{Sample OD (treated)}}{\text{Control OD (untreated)}} \times 100$$

The 50% cytotoxic concentration (CC<sub>50</sub>) values of the Cinnamon bark extract and corresponding silver nanoparticles were calculated by regression analysis. CC<sub>50</sub> is defined as the concentration required to reduce cell viability by 50%.

#### Infectivity Assay

Vero cells were treated with various concentrations of Cinnamon

bark extract (0, 31.25, 62.5, 125, 250, and 500 µg/ml) and corresponding nanoparticles (0, 1, 10, 50, 100, and 200 µg/ml) during and after influenza virus infection. For pre-penetration exposure, 10<sup>4</sup> TCID<sub>50</sub> virus suspension was incubated at 37°C with Cinnamon bark extract and its nanoparticles, and 100 µl of the mixture was then added to the Vero cells cultured in the 96-well microtiter plate. Cells were incubated for 2 h at 37°C under 5% CO<sub>2</sub>. Following incubation, the supernatant was removed and cells were washed with PBS. Thereafter, 100 µl of medium was added to each well. For post-penetration exposure, 10<sup>4</sup> TCID<sub>50</sub> virus suspension was added to the Vero cell culture and incubated for 2 h at 37°C under 5% CO<sub>2</sub>. Following incubation, cells were washed and 100 µl of Cinnamon bark extract and its nanoparticles was added to each well. Along with treated wells, virus-infected control and mock-infected control were also maintained. All plates were incubated for 48 h at 37°C. Then the MTT assay was carried out. The viability of infected and uninfected cells was determined from optical density values, and the percentage of protection was calculated using the following formula:

$$\frac{\text{Sample OD (virus infected and treated)} - \text{Control OD (virus infected)}}{\text{Control OD (mock infected)} - \text{Control OD (virus infected)}} \times 100$$

#### Statistical Analysis

All experiments of cytotoxicity and virus infectivity were conducted in triplicate and three independent experiments were carried out. Data are presented as the mean ± Standard deviation (SD). The data were evaluated statistically using one-way analysis of variance (ANOVA) to compare the difference in the means of treated and untreated samples. A *p*-value of <0.05 was considered to be significant. GraphPad Prism program (ver. 5.03) was used for determination of the IC<sub>50</sub> and CC<sub>50</sub> values.

## Results

### Synthesis of Cinnamon-Based AgNPs

Silver nanoparticles were synthesized using an aqueous extract of Cinnamon bark. When the extract was mixed with AgNO<sub>3</sub> solution and incubated at room temperature, change in color was observed within 5–6 h. The color of AgNPs synthesized using Cinnamon bark changed to dark brown. The change in color indicates the reduction of silver ions into silver particles.

### Characterization of Cinnamon-Based AgNPs

The synthesized silver nanoparticles were characterized by UV-Vis spectrophotometric analysis. In our study, absorption spectra of silver NPs formed from Cinnamon showed a single broad peak at 410 nm (Fig. 1). To get more information about the size and shape of the particles, the colloidal suspensions of AgNPs were diluted and analyzed using a scanning electron microscope. SEM analysis

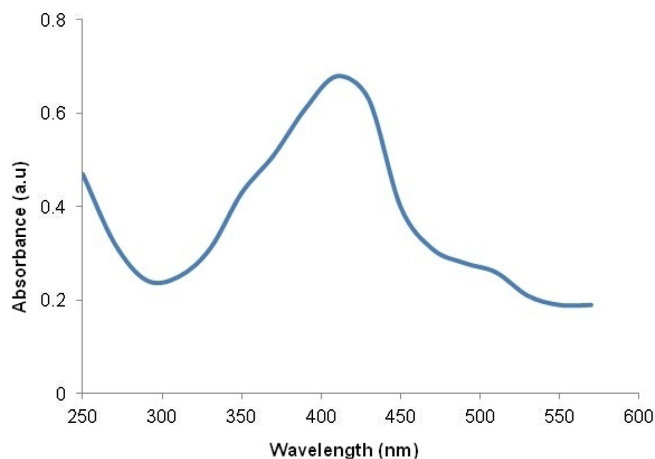


**Fig. 1.** UV-Vis spectral analysis of silver nanoparticles synthesized from bark extract of Cinnamon.

showed that the NPs were spherical in shape. The average size of Cinnamon-reduced NPs was approx. 42 nm, with size ranged from 25 to 55 nm (Fig. 2).

FTIR analysis was done to get information about the transformation of functional groups due to the reduction process. FTIR absorption spectra in the region of 500–4,000  $\text{cm}^{-1}$  of Cinnamon bark extract before and after reduction of silver ions are shown in Fig. 3. Absorbance peaks of Cinnamon bark extract were observed at 688, 1634, 2,077, and 3,445  $\text{cm}^{-1}$ . The Cinnamon-based silver NPs showed absorption peaks at 674, 1,637, and 3,433  $\text{cm}^{-1}$ . Comparison between FTIR spectra of Cinnamon and Cinnamon-based AgNPs revealed minor changes in magnitude and positions of the absorption peaks. The wavenumbers varied typically about  $\pm 1\text{--}15 \text{ cm}^{-1}$ .

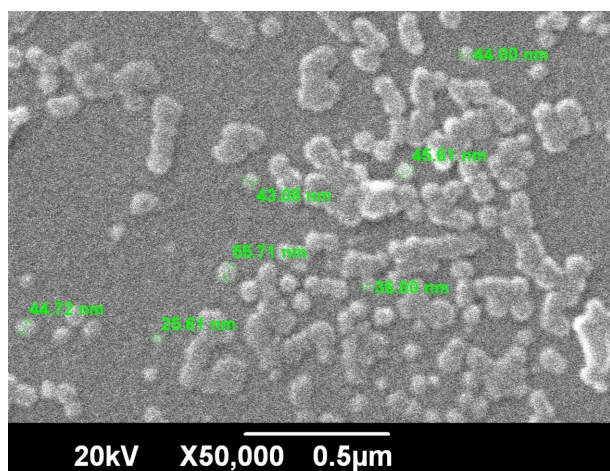


**Fig. 2.** SEM image of silver nanoparticles synthesized by bark extract of Cinnamon, at 50,000 $\times$  magnification.

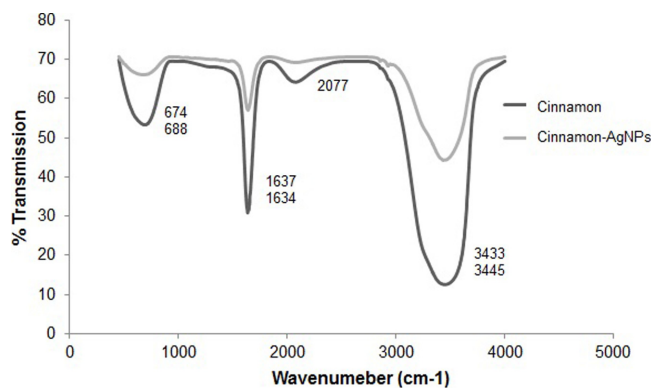


**Fig. 3.** FTIR spectrum analysis of Cinnamon bark extract before and after synthesis of silver nanoparticles.

### Cytotoxic Effect of Cinnamon and Cinnamon-Based AgNPs

Safety is one of the major prerequisites for any potential antiviral agent. Thus, the toxicity of the various concentrations of Cinnamon bark extract and Cinnamon bark-derived silver nanoparticles was tested in Vero cells in order to determine their safety profile. Vero cells were treated with various concentrations of Cinnamon bark extract and its nanoparticles (500, 250, 125, 62.5, 31.25, and 15.6  $\mu\text{g}/\text{ml}$ ). After 24 h incubation, cells were observed under a microscope. No cytopathic effects were found, showing that none of the tested concentrations of the Cinnamon extract and its nanoparticles were toxic to cells.

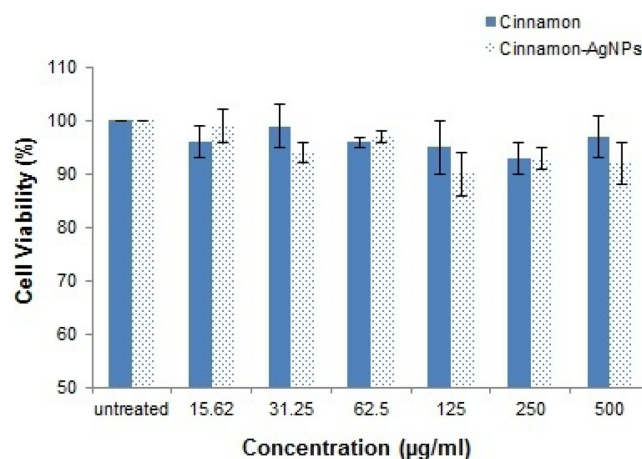


**Fig. 4.** Cytotoxicity effect of Cinnamon bark extract and its nanoparticles in Vero cells.

Cell viability was measured by MTT assay and the percentage of cell viability was calculated relative to the cell control. All the tested concentrations of Cinnamon and its nanoparticles showed insignificant toxicity to cells with  $p > 0.05$  (one-way ANOVA applied for statistical analysis).

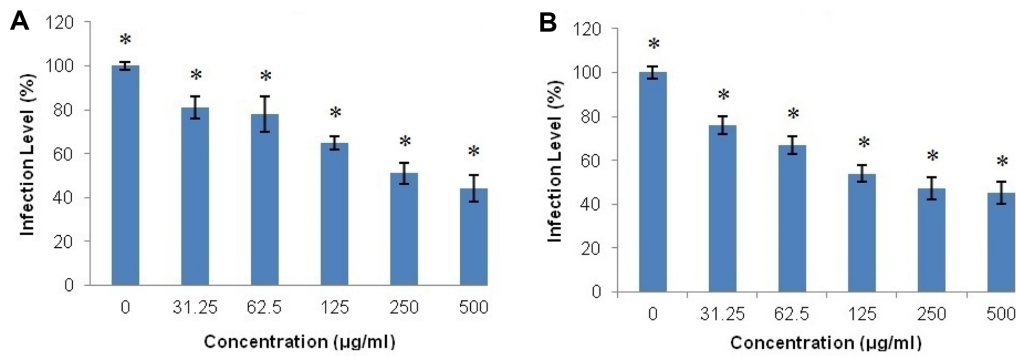


**Fig. 5.** Effect of Cinnamon bark extract on inhibition of H7N3 infection in Vero cells.

(A) Inhibition of infection when virus was incubated with extract for an hour prior to their introduction to cells. (B) Infection inhibition when cells were treated with extract after infection with virus. Tested concentrations indicating significant inhibition of infection are represented by an asterisk \* (at  $p < 0.05$  using one-way ANOVA). Representatives of three independent experiments conducted in triplicate are shown.

Furthermore, by means of MTT colorimetric assay, the viability of cells was also determined. In viable cells, the mitochondrial dehydrogenase reduces MTT to formazan. This conversion can be measured spectrophotometrically. It was confirmed by MTT assay that there was no significant difference in the viability of treated cells (Cinnamon bark extract and its AgNPs) and untreated control (Fig. 4). The  $CC_{50}$  of Cinnamon bark extract was 14.7 mg/ml, and the cytotoxicity of Cinnamon-derived silver nanoparticles was increased with  $CC_{50}$  of 4.9 mg/ml against Vero cells.  $CC_{50}$  values were greater than the highest concentration tested. In this case,  $CC_{50}$  was the theoretical value obtained by graphical extrapolation of the results.

#### Antiviral Activity of Cinnamon and Cinnamon-Based AgNPs

In order to determine the protective effects of Cinnamon

bark extract and its AgNPs, Vero cells were treated with five different non-cytotoxic concentrations of Cinnamon (31.25, 62.5, 125, 250, and 500 µg/ml) and its nanoparticles (1, 10, 50, 100, and 200 µg/ml). Influenza virus was incubated with Cinnamon and the corresponding NPs before infection to cells (pre-penetration exposure) and cells were treated with cinnamon extracts and its nanoparticles after infection with the virus (post-penetration exposure).

Antiviral activity of cinnamon bark extract showed that it was effective against influenza virus. All the tested concentrations of the extracts (31.25, 62.5, 125, 250, and 500 µg/ml) showed significant antiviral activity in comparison with the control, as shown in Figs. 5A and 5B. Comparison of the Cinnamon bark effectiveness against virus in pre-treatment and post-treatment exposures showed Cinnamon bark extract was more effective against

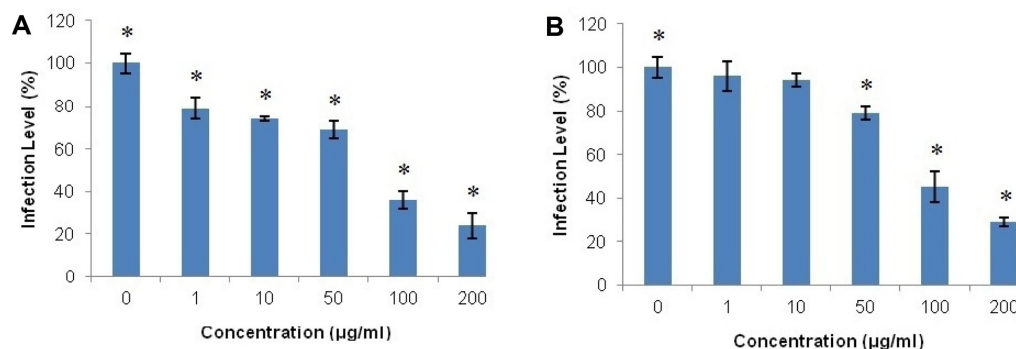


**Fig. 6.** Effect of Cinnamon bark-based silver nanoparticles on inhibition of H7N3 infection in Vero cells.

(A) Inhibition of infection when virus was incubated with NPs for an hour prior to their introduction to cells. One-way ANOVA showed significant inhibition at all concentrations, represented by asterisks \* (at  $p < 0.05$ ). (B) Infection inhibition when cells were treated with NPs after infection with virus. Higher concentrations (50, 100, and 200 µg/ml) indicating significant inhibition of viral infection are represented by asterisks \* (at  $p < 0.05$ ), whereas lower concentrations (1 and 10 µg/ml) showed  $p > 0.05$ , indicating insignificant inhibition of infection. Representatives of three independent experiments conducted in triplicate are shown.

viral infection when the virus was pre-treated with the extract before their introduction to cells ( $IC_{50}$  242  $\mu\text{g}/\text{ml}$ ) as compared with that of treatment of cells with extract after virus infection ( $IC_{50}$  316  $\mu\text{g}/\text{ml}$ ). Furthermore, at the high concentrations of 250 and 500  $\mu\text{g}/\text{ml}$ , the infection inhibition in pre-penetration and post-penetration exposures showed no noticeable difference of antiviral activity of Cinnamon bark extract, whereas at lower concentrations (31.250, 31.25, 62.5, and 125  $\mu\text{g}/\text{ml}$ ) extracts showed more efficient inhibition of virus infection when it was pre-incubated with virus prior to infection. The Cinnamon-derived NPs increased the antiviral activity of the Cinnamon, as evident in Figs. 6A and 6B. The concentration of NPs at which infectivity was inhibited by 50% ( $IC_{50}$ ) was 101  $\mu\text{g}/\text{ml}$  and 125  $\mu\text{g}/\text{ml}$  for treatment of cells during and after viral infection, respectively. The treatment of cells with Cinnamon NPs after viral infection did not show any significant inhibition ( $p$  values > 0.05) at lower concentrations (1 and 10  $\mu\text{g}/\text{ml}$ ). When virus was incubated with same concentrations of NPs prior to inoculating the cells, significant inhibition of the virus was observed. Higher concentrations of Cinnamon NPs (50, 100, and 200  $\mu\text{g}/\text{ml}$ ) showed statistically significant antiviral activity in both pre-penetration and post-penetration exposures. However, this effectiveness was increased when the virus was pretreated with the NPs prior to infection.

## Discussion

Avian influenza virus is a respiratory pathogen distributed throughout the world. It possesses the ability to switch to a new host and to escape antiviral measures [37]. Therefore, there is an urgent need to develop new antiviral agents for the treatment and control of influenza [56]. Medicinal plants have a variety of natural compounds having antiviral activity. Plant-based AgNPs can further improve the therapeutic applicability of plants and are a likely source of new antiviral agents [16]. These are safer and, because of their multivalent functions, less probable to encounter resistant viruses. Here, we report green synthesis of silver nanoparticles using Cinnamon bark and their application in inhibition of H7N3 infection.

Many researchers have explained the efficient method of green synthesis of silver NPs using various plant extracts. Our results are in agreement with Geethalakshmi and Sarada [7], who reported the formation of AgNPs within 5 h of incubation. Another study stated the reduction of silver ions to NPs within 8 min using *Ocimum sanctum* leaf extract [17]. The differences in the rate of bioreduction

may be due to variability in the plants used for synthesis of nanoparticles. The reduction was ascribed to the polysaccharides, phenolics, terpenoids, and flavone compounds present in the plant extract [19]. The procedure of bioreduction is not fully known and needs to be explored.

The optical absorption spectrum of metal NPs is highly influenced by the size and shape of nanoparticles [64]. Metal NPs ranging 2–100 nm show strong and broad peaks [4]. In our study, the absorption spectrum of silver NPs formed from Cinnamon showed a single broad peak at 410 nm. The number of peaks in the absorption spectra is a blueprint for the shape of the NPs. It has been shown that spherical nanoparticles generate a single peak. Broadening of the peak indicates that the particles are polydispersed [65]. Further SEM analysis confirmed that NPs were spherical in shape, and the average size of Cinnamon-reduced NPs was 42 nm with size ranged from 25 to 55 nm. Several reports have shown that the silver nanoparticles are generally spherical in shape and variable in size. Silver nanoparticles produced by *Morinda pubescens* and *Leptadenia reticulata* were 15–20 nm and 50–70 nm, respectively [6, 57]. The size and shape of the silver nanoparticles can have an impact on their application [12].

FTIR analysis was carried out to identify the possible potential biomolecules in the Cinnamon bark extract responsible for the reduction of silver ions to silver nanoparticles. The FTIR spectra of Cinnamon-based AgNPs revealed few changes in the position and magnitude of the bands. The band at 688  $\text{cm}^{-1}$  was shifted to a lower wave number at 674  $\text{cm}^{-1}$ , suggesting alkyl halides involvement in AgNP formation. After reduction of  $\text{AgNO}_3$ , the band at 1,634  $\text{cm}^{-1}$  characteristic of C=C- or aromatic groups vibrations showed increased transmittance and decreased absorbance, indicating these groups might be involved in stabilization and formation of the silver NPs. The band at 2,077  $\text{cm}^{-1}$  related to C=O stretching vibrations disappeared, which showed that the carbonyl functional group of aldehydes, ketones, and carboxylic acids might be involved in reduction of silver ions. The increased transmittance of the band at 3,445  $\text{cm}^{-1}$  corresponding to the NH group of amides or OH group of alcohol or phenol showed that these might be responsible for the formation of AgNPs. Previously, it has been reported that formation of AgNPs increased the transmittance of bands corresponding to NH and OH stretching [21, 38].

The tested concentrations of Cinnamon bark and its NPs did not show cytotoxic effect in Vero cells. There was no difference in cell number and morphological characteristics

between the treated and untreated cells. The MTT assay was performed to determine the cell viability, as the assay has a high sensitivity and rapid response as compared with lactate dehydrogenase and trypan blue exclusion assays [52]. The anti-influenza effects of Cinnamon and its NPs were evaluated in Vero cells. Although both Cinnamon and its corresponding silver nanoparticles inhibited H7N3 influenza virus infection in Vero cells, results showed the Cinnamon-based AgNPs are more effective against the virus.

Cinnamon has been used as medicine around the world because of its health benefits. The major constituents of Cinnamon are cinnamaldehyde, *trans*-cinnamaldehyde, cinnamic acid, essential oils, and eugenol. Study reported by Hayashi *et al.* [51] showed that *trans*-cinnamaldehyde of cinnamon could inhibit influenza A/PR/8 virus propagation in vitro and in vivo. In our study, incubation of virus with Cinnamon bark extract before influenza infection to cells reduced infectivity by up to 45% at a concentration of 500 µg/ml. It is therefore speculated that interaction of Cinnamon components with the virus possibly blocked HA function and resulted in inhibition of viral entry into the cell. In addition, treatment of cells with Cinnamon after viral entry also showed reduction of infection by up to 45% at a concentration of 500 µg/ml. It might be due to interactions of Cinnamon components with certain factors or pathways essential for viral replication.

We synthesized silver nanoparticles using Cinnamon bark for reduction of AgNO<sub>3</sub>. According to our results, biosynthesis of silver nanoparticles using Cinnamon enhanced the antiviral activity in both pre-penetration and post-penetration exposures. AgNPs showed more significant inhibition of viral infection when incubated with virus prior to infection, where the infection level was reduced by up to 24% at a concentration of 200 µg/ml. It has been reported that silver or gold nanoparticles exhibit antiviral activity against numerous viruses such as herpes simplex virus [25], hepatitis B [27], and H1N1 influenza A virus [48, 36]. Although the antiviral mechanism of action has not been determined, the antiviral activity of silver NPs against several types of viruses is likely due to binding of NPs to viral envelope glycoproteins, thereby hampering viral penetration into the host cell [27, 62]. It has been shown that silver nanoparticles inhibit HIV adsorption to the host cells [23]. In our study, treatment of cells with Cinnamon-based AgNPs after viral entry reduced infection by up to 29% at a concentration of 200 µg/ml. It revealed that besides the interaction with viral glycoproteins directly, NPs may get access into the cell and show their antiviral activity through interactions with the viral genome (RNA

or DNA), cellular factors, or pathways of host cells that are essential for viral replication [48].

In the present study, silver nanoparticles were successfully developed by a green synthetic approach using bark extract of Cinnamon. Cinnamon-reduced silver nanoparticles exhibited an enhancement of antiviral activity against H7N3 influenza virus as compared with Cinnamon bark aqueous extract, in both pre-penetration and post-penetration exposures. Cinnamon and its corresponding nanoparticles were found nontoxic against Vero cells. The safe and multi-target benefits of plant-based silver nanoparticles give hope where there are no treatments for highly mutating viruses. The mechanism of action of nanoparticles needs to be further investigated to develop better antiviral therapeutics. In vivo studies to show the effectiveness of Cinnamon-based nanoparticles against influenza are under way.

## Acknowledgments

We are thankful to the Higher Education Commission, Pakistan for funding these studies. We acknowledge Attaur-Rahman School of Applied Biosciences (ASAB), National University of Sciences and Technology (NUST) for providing lab facilities and support to accomplish this work. We sincerely thank the School of Chemical and Material Engineering (SCME), for SEM and FTIR analyses. We would like to thank Dr. Jawad Nazir from Microbiology Department at University of Veterinary and Animal Sciences for giving the vero cell line, and Mr. Abdul Rehman from Poultry Research Institute for providing the influenza virus for our studies.

## References

1. Ankamwar B, Chaudhary M, Sastry M. 2005. Gold nanotriangles biologically synthesized using tamarind leaf extract and potential application in vapor sensing. *Syn. React. Inorg. Met.* **35**: 19-26.
2. Ankanna S, Prasad TNVKV, Elumalai EK, Savithamma N. 2010. Production of biogenic silver nanoparticles using *Boswellia ovalifoliolata* stem bark. *Dig. J. Nanomater. Biostruct.* **5**: 369-372.
3. Bae CH, Nam SH, Park SM. 2002. Formation of silver nanoparticles by laser ablation of a silver target in NaCl solution. *Appl. Surf. Sci.* **197**: 628-634.
4. Baram-Pinto D, Shukla S, Gedanken A, Sarid R. 2010. Inhibition of HSV-1 attachment, entry, and cell-to-cell Spread by functionalized multivalent gold nanoparticles. *Small* **6**: 1044-1050.

5. Baram-Pinto D, Shukla S, Perkas N, Gedanken A, Sarid R. 2009. Inhibition of herpes simplex virus type 1 infection by silver nanoparticles capped with mercaptoethane sulfonate. *Bioconjug. Chem.* **20**: 1497-1502.
6. Chandran SP, Chaudhary M, Pasricha R, Ahmad A, Sastry M. 2006. Synthesis of gold nanotriangles and silver nanoparticles using *Aloe vera* plant extract. *Biotechnol. Prog.* **22**: 577-583.
7. Choi YK, Ozaki H, Webby RJ, Webster RG, Peiris JS, Poon L, et al. 2004. Continuing evolution of H9N2 influenza viruses in Southeastern China. *J. Virol.* **78**: 8609-8614.
8. Cralg, WJ. 1999. Health-promoting properties of common herbs. *Amer. J. Clin. Nutr.* **70**: 4915-4995.
9. Da Costa AO, De Assis MC, Marques EA, Plotkowski MC. 1999. Comparative analysis of three methods to assess viability of mammalian cells in culture. *Biocell* **23**: 65-72.
10. De Clercq E. 2004. Antiviral drugs in current clinical use. *J. Clin. Virol.* **30**: 115-133.
11. Elechiguerra JL, Burt JL, Morones JR. 2005. Interaction of silver nanoparticles with HIV-1. *J. Nanobiotechnology* **3**: 1-10.
12. Esteban D. 2010. Mechanisms of viral emergence. *Vet. Res.* **41**: 38.
13. Fayaz AM, Ao Z, Girilal M, Chen L, Xiao X, Kalaichelvan P, Yao X, et al. 2012. Inactivation of microbial infectiousness by silver nanoparticles-coated condom: a new approach to inhibit HIV- and HSV-transmitted infection. *Int. J. Nanomedicine* **7**: 5007-5018.
14. Ferguson NM, Cummings DAT, Cauchemez S. 2005. Strategies for containing an emerging influenza pandemic in Southeast Asia. *Nature* **437**: 209-214.
15. Fouchier RA, Schneeberger PM, Rozendaal FW, Broekman JM, Kemink SA, Munster V, et al. 2004. Avian influenza A virus (H7N7) associated with human conjunctivitis and a fatal case of acute respiratory distress syndrome. *Proc. Natl. Acad. Sci. USA* **101**: 1356-1361.
16. Galdiero S, Falanga A, Cantisani M, Ingle A, Galdiero M, Rai M. 2014. Silver nanoparticles as novel antibacterial and antiviral agents, pp. 565-594. In: *Frontiers of Nanomedical Research*. World Scientific Publishing, Singapore.
17. Gan PP, Li SF. 2012. Potential of plant as a biological factory to synthesize gold and silver nanoparticles and their applications. *Rev. Environ. Sci. Biotechnol.* **11**: 169-206.
18. Geethalakshmi R, Sarada DVL. 2010. Synthesis of plant-mediated silver nanoparticles using *Trianthema decandra* extract and evaluation of their anti-microbial activities. *Int. J. Eng. Sci. Technol.* **2**: 970-975.
19. Ha Y, Stevens DJ, Skehel JJ, Wiley DC. 2001. X-ray structures of H5 avian and H9 swine influenza virus hemagglutinins bound to avian and human receptor analogs. *Proc. Natl. Acad. Sci. USA* **98**: 11181-11186.
20. Hayashi K, Imanishi N, Kashiwayama Y, Kawano A, Terasawa K, Shimada Y, Ochiai H. 2007. Inhibitory effect of cinnamaldehyde, derived from *Cinnamomi cortex*, on the growth of influenza A/PR/8 virus in vitro and in vivo. *Antiviral Res.* **74**: 1-8.
21. Huang J, Chen C, He N. 2007. Biosynthesis of silver and gold nanoparticles by novel sun dried *Cinnamomum camphora* leaf. *Nanotechnology* **18**: 105-106.
22. Kinoshita E, Hayashi K, Katayama H, Hayashi T, Obata A. 2012. Anti-influenza virus effects of elderberry juice and its fractions. *Biosci. Biotechnol. Biochem.* **76**: 1633-1638.
23. Klaus T, Joerger R, Olsson E, Granqvist CG. 1999. Silver-based crystalline nanoparticles, microbially fabricated. *Proc. Natl. Acad. Sci. USA.* **96**: 13611-13614.
24. Ko HC, Wei BL, Chiou WF. 2006. The effect of medicinal plants used in Chinese folk medicine on RANTES secretion by virus-infected human epithelial cells. *J. Ethnopharmacol.* **107**: 205-210.
25. Konishi Y, Ohno K, Saitoh N, Nomura T, Nagamine S, Hishida H, et al. 2007. Bioreductive deposition of platinum nanoparticles on the bacterium *Shewanella algae*. *J. Biotechnol.* **128**: 648-653.
26. Kubo T, Nishimura H. 2007. Antipyretic effect of Mao-to, a Japanese herbal medicine, for treatment of type A influenza infection in children. *Phytomedicine* **14**: 96-101.
27. Kwon HJ, Kim HH, Yoon SY, Ryu YB, Chang JS, Cho KO, et al. 2010. In Vitro inhibitory activity of *Alpinia katsumadai* extracts against influenza virus infection and hemagglutination. *Virol. J.* **7**: 307.
28. Lara HH, Garza-Trevino EN, Ixtepan-Turrent L, Singh DK. 2011. Silver nanoparticles are broad-spectrum bactericidal and virucidal compounds. *J. Nanobiotechnology* **9**: 30.
29. Lee JB, Miyake S, Umetsu R, Hayashi K, Chijimatsu T, Hayashi T. 2012. Anti-influenza A virus effects of fructan from Welsh onion (*Allium fistulosum* L.). *Food Chem.* **134**: 2164-2168.
30. Liu YC, Lin LH. 2004. New pathway for the synthesis of ultrafine silver nanoparticles from bulk silver substrates in aqueous solutions by sonoelectrochemical methods. *Electrochem. Commun.* **6**: 1163-1168.
31. Lu L, Sun RW, Chen RWR, Hui CK, Ho CM, Luk JM, et al. 2008. Silver nanoparticles inhibit hepatitis B virus replication. *Antivir. Ther.* **13**: 253-262.
32. Mallick K, Witcomb MJ, Scurrilla MS. 2005. Self-assembly of silver nanoparticles in a polymer solvent: formation of a nanochain through nanoscale soldering. *Mater. Chem. Phys.* **90**: 221-224.
33. Mallikarjun K, Narsimha G, Dillip G, Praveen B, Shreedhar B, Lakshmi S. 2011. Green synthesis of silver nanoparticles using *Ocimum* leaf extract and their characterization. *Dig. J. Nanomater. Biostruct.* **6**: 181-186.
34. Mantani N, Andoh T, Kawamata H, Terasawa K, Ochiai H. 1999. Inhibitory effect of *Ephedrae herba*, an oriental traditional medicine, on the growth of influenza A/PR/8 virus in MDCK cells. *Antiviral Res.* **44**: 193-200.
35. Jancy ME, Inbathamizh L. 2012. Green synthesis and characterization of nano silver using leaf extract of *Morinda*

- pubescens*. *Asian J. Pharm. Clinical Res.* **5**: 159-162.
36. Mori Y, Ono T, Miyahira Y, Nguyen VQ, Matsui T, Ishihara M. 2013. Antiviral activity of silver nanoparticles/chitosan composites against H1N1 influenza A virus. *Nanoscale Res. Lett.* **8**: 93.
  37. Nair B, Pradeep T. 2002. Coalescence of nanoclusters and formation of submicron crystallites assisted by *Lactobacillus* strains. *Cryst. Growth Des.* **2**: 293-298.
  38. Noh HJ, A-Rang I, Kim H. 2012. Antimicrobial activity and increased freeze-drying stability of sialyllactose-reduced silver nanoparticles using sucrose and trehalose. *J. Nanosci. Nanotechnol.* **12**: 3884-3895.
  39. Papp I, Sieben C, Ludwig K, Roskamp M, Bottcher C, Schlecht S, et al. 2010. Inhibition of Influenza virus infection by multivalent Sialic-acid-functionalized Gold nanoparticles. *Small* **6**: 2900-2906.
  40. Parak WJ, Gerion D, Pellegrino T, Zanchet D, Micheel C, Williams SC, et al. 2003. Biological applications of colloidal nanocrystals. *Nanotechnology* **14**: 15-27.
  41. Peyre M, Fusheng G, Desvaux S, Roger F. 2009. Avian influenza vaccines: a practical review in relation to their application in the field with a focus on the Asian experience. *Epidemiol. Infect.* **137**: 1-21.
  42. Poland GA, Jacobson RM, Ovsyannikova IG. 2009. Influenza virus resistance to antiviral agents: a plea for rational use. *Clin. Infect. Dis.* **48**: 1254-1256.
  43. Prathap SC, Chaudhary M, Pasricha R, Ahmad A, Sastry M. 2006. Synthesis of gold nanotriangles and silver nanoparticles using *Aloe vera* plant extract. *Biotechnol. Prog.* **22**: 577-583.
  44. Reed LJ, Muench H. 1938. A simple method of estimating fifty percent endpoints. *Am. J. Hyg.* **27**: 493-497.
  45. Rogers JV, Parkinson CV, Choi YW, Speshock JL, Hussain SM. 2008. A preliminary assessment of silver nanoparticle inhibition of monkeypox virus plaque formation. *Nanoscale Res. Lett.* **3**: 129-133.
  46. Sandmann G, Dietz H, Plieth W. 2000. Preparation of silver nanoparticles on ITO surfaces by a double-pulse method. *J. Electroanal. Chem.* **491**: 78-86.
  47. Shankar SS, Ahmad A, Rai A, Sastry M. 2004. Rapid synthesis of Au, Ag and bimetallic Au core-Ag shell nanoparticles by using neem (*Azadirachta indica*) leaf broth. *J. Colloid. Interface Sci.* **275**: 496-502.
  48. Shankar SS, Rai A, Ahmad A, Sastry M. 2005. Controlling the optical properties of lemongrass extract synthesized gold nanotriangles and potential application in infrared-absorbing optical coatings. *Chem. Mater.* **17**: 566-572.
  49. Shivshankar S, Ahmad A, Sastry M. 2003. Geranium leaf assisted biosynthesis of silver nanoparticles. *Biotechnol. Prog.* **19**: 1627-1631.
  50. Sivaraman SK, Elango I, Kumar S, Santhanam V. 2009. A green protocol for room temperature synthesis of silver nanoparticles in seconds. *Curr. Sci.* **97**: 1055-1059.
  51. Skehel JJ, Wiley, DC. 2000. Receptor binding and membrane fusion in virus entry: the influenza hemagglutinin. *Ann. Rev. Biochem.* **69**: 531-569
  52. Smetana AB, Klabunde KJ, Sorensen CM. 2005. Synthesis of spherical silver nanoparticles by digestive ripening, stabilization with various agents, and their 3-D and 2-D superlattice formation. *J. Colloid. Interface Sci.* **284**: 521-526.
  53. Sondi I, Salopek-Sondi B. 2004. Silver nanoparticles as antimicrobial agent: a case study on *E. coli* as a model for gram-negative bacteria. *J. Colloid. Interface Sci.* **275**: 177-182.
  54. Speshock JL, Murdock RC, Braydich-Stolle LK, Schrand AM, Hussain SM. 2010. Interaction of silver nanoparticles with Tacaribe virus. *J. Nanobiotechnology* **8**: 19.
  55. Sriwilajaroen N, Fukumoto S, Kumagai K, Hiramatsu H, Odagiri T, Tashiro M, Suzuki Y. 2012. Antiviral effects of *Psidium guajava* Linn (guava) tea on the growth of clinical isolated H1N1 viruses: its role in viral hemagglutination and neuraminidase inhibition. *Antivir. Res.* **94**: 139-146.
  56. Sun L, Singh AK, Vig K, Pillai SR, Singh SR. 2008. Silver nanoparticles inhibit replication of respiratory syncytial virus. *J. Biomed. Nanotechnol.* **4**: 149-158.
  57. Swamy MK, Sudipta KM, Jayanta K. Balasubramanya S. 2015. The green synthesis, characterization, and evaluation of the biological activities of silver nanoparticles synthesized from *Leptadenia reticulata* leaf extract. *Appl. Nanosci.* **5**: 73-81.
  58. Vorobyova SA, Lesnikovich AI, Sobal NS. 1999. Preparation of silver nanoparticles by interphase reduction. *Colloids Surf. A: Physicochem. Eng. Aspects* **152**: 375-379.
  59. Webster RG, Bean WJ, German OT, Chambers TM, Kawaoka Y. 1992. Evolution and ecology of influenza A viruses. *Microbiol. Rev.* **56**: 152-179.
  60. Wei D, Qian W. 2008. Facile synthesis of Ag and Au nanoparticles utilizing chitosan as a mediator agent. *Colloids Surf. B Biointerface* **62**: 136-142.
  61. Willner I, Baron R, Willner B. 2006. Growing metal nanoparticles by enzymes. *Adv. Mater.* **18**: 1109-1120.
  62. Won JN, Lee SY, Song DS Poo H. 2013. Antiviral activity of the plant extracts from *Thuja orientalis*, *Aster spathulifolius*, and *Pinus thunbergii* against influenza virus A/PR/8/34. *J. Microbiol. Biotechnol.* **23**: 125-130.
  63. Xia Y, Halas NJ. 2005. Shape-controlled synthesis and surface plasmonic properties of metallic nanostructures. *MRS Bull.* **30**: 338-348.
  64. Xiang DX, Chen Q, Pang L, Zheng CL. 2011. Inhibitory effects of silver nanoparticles on H1N1 influenza A virus in vitro. *J. Virol. Methods* **178**: 137-142.
  65. Yu DG. 2007. Formation of colloidal silver nanoparticles stabilized by Na<sup>+</sup>-poly (-glutamic acid) silver nitrate complex via chemical reduction process. *Colloids Surf. B Biointerfaces* **59**: 171-178.